IEEE Access
Multidisciplinary | Rapid Review | Open Access Journal

Received June 21, 2019, accepted July 14, 2019, date of publication August 15, 2019, date of current version September 9, 2019.

Digital Object Identifier 10.1109/ACCESS.2019.2935505

Efficient Sidelink Identity Detection and Frequency Ambiguity Resolution for LTE-D2D Communications

YONG-AN JUNG[1], JONG-HONG PARK[2], AND YOUNG-HWAN YOU[1]
[1]Department of Computer Engineering, Sejong University, Seoul 05006, South Korea
[2]Autonomous IoT Research Center, Korea Electronics Technology Institute (KETI), Seongnam 13509, South Korea

Corresponding author: Young-Hwan You (yhyou@sejong.ac.kr)

This work was supported in part by the Unmanned Vehicles Advanced Core Technology Research and Development Program of the National Research Foundation of Korea (NRF), in part by the Unmanned Vehicle Advanced Research Center (UVARC) funded by the Ministry of Science and ICT, South Korea, under Grant NRF-2017M1B3A2A01049997, and in part by the Basic Science Research Program of NRF funded by the Ministry of Education under Grant NRF-2018R1D1A1B07048819.

ABSTRACT Device-to-device (D2D) communication is a key enabler to facilitate the realization of the Internet of Things (IoT) in which devices directly communicate with each other. One of the major challenges in the D2D network is robust and low-cost synchronization for ultra-reliable low latency communication. To address this issue, this paper presents an efficient frequency ambiguity resolution and sidelink synchronization identity detection scheme for D2D communications in the long term evolution system. To perform low-cost joint detection, the proposed method is based on the grouping of the primary sidelink synchronization sequence (PSSS) subcarriers. The PSSS subcarriers are grouped into a number of subsets wherein the phase difference between the PSSS subcarriers is approximately a multiple of $\pi/2$. Numerical analysis is performed to present the relationship between detection probability and design parameter. Simulations show that the proposed method has the same performance as the existing detection method, with significantly reduced computational complexity.

INDEX TERMS Device-to-device communication, Internet of Things, long-term evolution, sidelink synchronization, synchronization signal.

I. INTRODUCTION

Long term evolution (LTE) is an attractive technology to be applied for a variety of wireless applications due to its ability to deliver high data rates with the reliable quality of service (QoS), which has been standardized by the third generation partnership project (3GPP) [1]. With the rapid development of cellular and IP networks, the ultimate communications infrastructure for the Internet of things (IoT) has been realized. The all-IP based architecture of LTE-Advanced (LTE-A) cellular networks makes it ideal for IoT applications. Recently, cellular IoT solutions such as narrowband IoT and device-to-device (D2D) communications have been considered as a key component in existing and future cellular LTE-A networks [2]–[5]. D2D communication is considered as an appealing technology for various IoT domains such as smart metering, industrial automation and control, remote manufacturing, and healthcare [6].

Among a variety of communication technologies that exist within the IoT, D2D communication allows user equipments (UEs) close to each other to communicate using a direct link, and can be operated as an underlay to LTE-A networks by sharing the scarce radio resources [7], [8]. In the D2D based IoT network, ultra-reliable low latency communication (URLLC) is an increasingly important aspect of wireless connectivity. To realize the URLLC requirement, it is a challenging task to acquire fast network connectivity and maintain the synchronization especially for out-of-network coverage scenarios, wherein the D2D devices have to synchronize with each other. To end this, the D2D device has not only to resolve symbol timing error and frequency ambiguity but also to detect the sidelink synchronization identity (SSID) [9]–[19]. A series of process of acquiring timing and frequency synchronization together with SSID of D2D devices is called as initial cell search. Due to the sensitivity of

The associate editor coordinating the review of this article and approving it for publication was Faisal Tariq.

orthogonal frequency division multiplexing (OFDM) to time and frequency misalignments, there is a need for reliable cell search procedure by which the D2D device determines time and frequency parameters so that the orthogonality of subcarriers can be maintained. Most of the existing synchronization methods are designed for downlink (DL) detection and are not the best solution for sidelink synchronization, but they can be applied to the D2D scenario [14]–[22]. A sidelink identity is acquired by detecting the SSID message transmitted through the synchronization signals such as primary sidelink synchronization signal (PSSS) and secondary sidelink synchronization signal (SSSS) [8]. During the first step of the initial cell search procedure, the D2D device exploits the redundant cyclic prefix (CP) to find the fractional frequency offset (FFO) and initial symbol timing offset (STO) [9]–[12]. In the second step, the PSSS is used to retrieve the SSID and detect integer frequency offset (IFO) [13]–[19]. After the completion of this stage, the SSSS is identified to determine the frame boundary and the sidelink ID (SID) [20]–[22].

In [12]–[14], the PSSS estimation method has been proposed to be performed in the time domain. One drawback of this strategy is that the detection accuracy depends on the existence of IFO. To solve this issue, the works in [15]–[19] have presented the PSSS detection scheme in the frequency domain. In [15], [16], a joint detection of the SSID and IFO during the PSSS-matching process was presented, which is accomplished observing the cross-correlation between the received PSSS and the original PSSS. With this detection strategy, the SSID and IFO can be jointly estimated employing the correlation banks for a large number of hypotheses, which requires a large amount of computational complexity. Maximum likelihood (ML) detection has been effectively used to estimate IFO [17], based upon the minimum mean-square-error criterion reduced-rank representation of the channel frequency response (CFR). At the cost of computational complexity, the ML estimator can realize optimal detection of IFO. To reduce the computational processing, a sequential SSID and IFO estimation scheme was developed exploiting the symmetric property of the PSSS [18], [19]. With the central symmetry property of the PSSS, it avoids the need to acquire the SSID. Therefore, such a design can decouple the SSID and IFO detection into two sequential tasks, while it suffers from longer processing delay and is vulnerable to the presence of STO, degrading its detection efficiency. Thus, it is of significant interest to develop accurate detection algorithm while reducing the complexity of D2D devices.

In this paper, we propose an efficient SSID and IFO detection method for D2D communications in the LTE system. To this end, the set of differential PSSS subcarriers is divided into a number of groups, each of which is represented by one group subcarrier. The proposed method that is based on partitioning of differential PSSS subcarriers facilitates low-complexity detection of SSID and IFO by performing group-wise correlation between received PSSS subcarriers and one representative PSSS subcarrier in subset. To investigate the effectiveness of the proposed joint estimation scheme, the probability of detection failure is analytically derived. It is shown that the processing burden of the proposed estimation scheme is considerably decreased while offering acceptable performance when compared to the conventional detection methods.

The rest of this paper is structured as follows. Next section presents the signal model and synchronization signal for the LTE-D2D communication. In Section III, the conventional detection methods using differential correlation are addressed. A computationally effective detection method for the LTE-D2D system is presented in Section IV. In Section V, the effectiveness of the proposed joint detection scheme is demonstrated by computer simulations. Finally, conclusions are drawn in Section VI.

II. SYSTEM DESCRIPTION

A. SIDELINK SYNCHRONIZATION PROCEDURE

In an LTE D2D network, a series of process of acquiring timing and frequency synchronization together with SSID is called as initial synchronization. To this end, the PSSS and SSSS sequences are periodically transmitted from the UE acting as a synchronization source. The initial synchronization procedure mainly comprises three steps. In the first step, initial STO and FFO estimation is accomplished in the time domain by using redundant information from the CP. After FFO compensation and CP extraction, the time-sampled OFDM signal is converted into the frequency domain by means of a fast Fourier transform (FFT). During the second stage, the SSID is retrieved together with the IFO detecting the PSSS, which can be accomplished in the time or frequency domain. Once these two steps are finished, the frame boundary and the SID is identified detecting the SSSS, thus recovering the radio frame timing for the D2D transmission.

B. SYNCHRONIZATION SIGNAL

Let us consider the sidelink of an LTE system operating in frequency division duplex mode. The period of one LTE radio frame is 10ms. Each frame is made up of 10 subframes of 1ms each, which is further divided into two equally sized slots of length 0.5ms. Every subframe includes 14 single-carrier frequency division multiple access (SC-FDMA) symbols for normal CP, while 12 SC-FDMA symbols are contained in the case of extended CP. In contrast to LTE DL, the D2D sidelink uses a pair of PSSS and SSSS, which are transmitted in two consecutive OFDM symbols every 40ms. An LTE sidelink system can support 336 different SSIDs numbered by $N_{ID} \in \{0, 1, 2, \cdots, 335\}$. These SSIDs are grouped into two sets depending on in-network and out-of-coverage scenarios, which are indexed as $\{0, 1, 2, \cdots, 167\}$ and $\{168, 169, \cdots, 335\}$, respectively. The PSSS is generated based on Zadoff-Chu (ZC) sequence that belongs to the class of constant amplitude zero autocorrelation sequences. The ZC root sequence index u_i $(i = 0, 1)$ is used to represent two sets corresponding to in-network and out of

network cases. From [1], $u_0 = 26$ for $N_{ID} \leq 167$ and $u_1 = 37$ otherwise. In frequency domain, the PSSS is constructed from a ZC sequence of length 63, with the middle element punctured to avoid transmitting on the DC subcarrier. Therefore, the DC subcarrier and the rest of the subcarriers in the symbols where the PSSS is present are zero-padded, leading to $N_p = 62$ non-zero PSSS subcarriers surrounding the DC subcarrier symmetrically, where N_p is the number of PSSS subcarriers. Two PSSS sequences are generated to have good periodic autocorrelation and cross-correlation properties [1]

$$P_i(k) = \begin{cases} e^{-j\pi u_i(k+31)(k+32)/63}, & k \in \mathcal{P} \\ 0, & \text{otherwise}, \end{cases} \tag{1}$$

where $\mathcal{P} = \{k | -N_p/2 \leq k \leq N_p/2, k \neq 0\}$ denotes the set of PSSS subcarrier indices. The SSSS sequences are mainly used to recognize the 168 SIDs, which are based on maximum length sequences. Each SSSS is generated by interleaving two length-31 scrambled and cyclically shifted binary phase-shift keying sequences $s_0^{(w_0)}(b)$ and $s_1^{(w_1)}(b)$, with $b = 0, 1, \cdots, N_p/2 - 1$.

C. SIGNAL MODEL

We assume that the synchronization signals are transmitted without discrete Fourier transform (DFT) precoding [8]. Thus, let us consider an OFDM system that employs N subcarriers and N_g guard interval (GI) samples with time durations of T and T_g, respectively. After performing an N-point inverse FFT (IFFT) on the information symbols, the last N_g samples of each OFDM symbol comprised of N samples are copied and appended at the beginning of the OFDM symbol. Thus, one effective OFDM symbol with time duration of $N_u T_s$ is generated, where T_s is the sampling time interval and $N_u = N + N_g$. The v-th time-domain sample during the q-th period $x_q(v)$, $v = -N_g, -N_g + 1, \cdots, N - 1$, can be written by

$$x_q(v) = \sum_{k=-N/2}^{N/2-1} X_q(k) e^{j2\pi kv/N} \tag{2}$$

where $X_q(k)$ is the frequency-domain signal at the k-th subcarrier in the q-th duration and the half subcarrier frequency shift for the SC-FDMA uplink signal is omitted for notational convenience. The remaining $X_q(k)$'s except for the synchronization signal are DFT-precoded signals. The continuous-time baseband signal transmitted is expressed as

$$x(t) = \sum_{q=-\infty}^{\infty} \sum_{k=-N/2}^{N/2-1} X_q(k) e^{j2\pi k(t-T_g-qT_u)/(NT_s)} u(t - qT_u) \tag{3}$$

where $T_u = T + T_g$ and $u(t)$ is the shaping pulse that takes the value $u(t) = 1$ for $0 \leq t < T_u$ and $u(t) = 0$ otherwise.

The time-domain signal is transmitted over a multipath fading channel with additive white Gaussian noise (AWGN) and the received signal is down-converted to baseband at the UE terminal. Since the frequency of the local oscillator f_c' is not exactly equal to the received carrier frequency f_c, there will be a frequency offset $f_c' - f_c$ in Hz. Since the FFO marginally affects the performance of the IFO detector like the existing approaches [17]–[19], we consider the scenario where the FFO is completely available at the receiver. With these implications in mind, the time-domain received signal can be given by

$$r(t) = e^{j2\pi(f_c'-f_c)t} x(t) \otimes h(t) + z(t) \tag{4}$$

where $\otimes$ denotes the linear convolution operator, $h(t)$ is the channel impulse response (CIR), and $z(t)$ is a zero-mean AWGN process. After FFO compensation, the symbol timing is recovered to remove the GI. We assume that there is a residual STO τ due to the presence of highly dispersive channels [9]. Without losing generality, we consider only integer-valued τ because any fractional STO can be incorporated into the CIR. In the presence of the STO τ, the sampling of OFDM symbol q is shifted from the optimal position and done at time instants $t = qT_u + vT_s + \tau T_s$. Thus, the time-domain signal during the q-th period $y_q(v)$, $v = -N_g, -N_g + 1, \cdots, N - 1$, appears as [13]

$$y_q(v) = e^{jq\epsilon N_g \rho} e^{j\epsilon(v-\tau)\rho} \sum_{p=1}^{L} h_q(p) x_q(v - \tau_p - \tau) + z_q(v) \tag{5}$$

where $\rho = 2\pi/N$, ϵ denotes the normalized IFO with respect to the subcarrier spacing $\Delta f = 1/(NT_s)$, $x_q(v)$ is the v-th sample over the q-th symbol period, $h_q(p)$ is the discrete CIR with L resolvable paths, τ_p is the delay of the p-th path, and $z_q(v)$ is the contribution of a zero-mean AWGN.

For notational convenience, we consider the situation where the PSSS is transmitted without DFT precoding on the l-th OFDM symbol, i.e., $X_l(k) = P_i(k)$. After extracting the CP, the FFT operation during the l-th symbol period transforms the time-domain sample $y_l(v)$ into

$$Y_l(k) = H_l(k - \epsilon) P_i(k - \epsilon) e^{-j(k-\epsilon)\tau\rho} e^{jl\epsilon N_g \rho} + Z_l(k), \quad k \in \mathcal{P} \tag{6}$$

where $H_l(k)$ denotes the CFR over the l-th period and $Z_l(k)$ is the frequency-domain representation of $z_q(v)$ with variance σ_Z^2.

III. CONVENTIONAL SSID AND IFO DETECTION SCHEMES

The SSID and IFO estimation is generally performed in a non-coherent manner since the the channel state information has not been known during the synchronization phase. To lessen the impact of the channel distortion and symbol timing error on the detection performance, the differential correlation between neighboring subcarriers of the received PSSS over the l-th period is written as

$$\begin{aligned} \bar{Y}_l(k) &= Y_l(k) Y_l^*(k-1) \\ &= |H_l(k-\epsilon)|^2 D_i(k-\epsilon) e^{j\tau\rho} + \bar{Z}_l(k), \quad k \in \mathcal{D} \end{aligned} \tag{7}$$

where $(\cdot)^*$ means the complex conjugation, $D_i(k) = P_i(k) P_i^*(k-1)$ is the differential relation from two adjacent PSSS

subcarriers, $\mathcal{D} = \{k | -N_p/2+1 \le k \le -1, 2 \le k \le N_p/2\}$, and $\bar{Z}_l(k)$ is the contribution to AWGN given by

$$\begin{aligned}\bar{Z}_l(k) &= H_l(k-\epsilon)X_l(k-\epsilon)Z_l^*(k-1)e^{-j(k-\epsilon)\tau\rho}e^{jl\epsilon N_g\rho} \\ &\quad + H_l^*(k-\epsilon-1)X_l^*(k-\epsilon-1)Z_l(k)e^{j(k-\epsilon)\tau\rho}e^{-jl\epsilon N_g\rho} \\ &\quad + Z_l(k)Z_l^*(k-1). \end{aligned} \tag{8}$$

Since $P_i(k)$ is central-symmetric around DC, it follows that $D_i(k) = D_i^*(-k+1)$ for $k \in [2, N_p/2]$. The SSID and IFO detection can be performed in a joint or sequential manner [15]–[19].

A. JOINT IFO AND SSID DETECTION (JISID) SCHEME

A joint detection scheme using central-symmetric property of the ZC sequence is widely used in the LTE system [15]–[17]. We may express the objective function $\Phi_p(m, n)$ with respect to symmetric-conjugate differential correlation

$$\Phi_a(m, n) = \sum_{k\in\mathcal{D}} \bar{Y}_l(k+m)D_n^*(k) \tag{9}$$

where m is the hypothesized IFO and n is the indicator of the ZC root sequence index. By searching the maximum of $\Phi_a(m, n)$ subject to m and n, the SSID and IFO joint detector has the following form [17]

$$(\hat{\epsilon}, \hat{n}) = \underset{|m|\le M, n\in\{0,1\}}{\arg\max} \ \Re\{\Phi_a(m, n)\} \tag{10}$$

where M is the finite number of possibilities of ϵ and $\Re\{x\}$ is the real term of the complex number x. Although this design can reduce the number of complex-valued multiplications by half, it still requires much computational complexity. Another disadvantage of the JISID scheme is that a loss of autocorrelation property of the original PSSS gives rise to similar peaks for different IFO trials and degrades its performance.

B. SEQUENTIAL IFO AND SSID DETECTION (SISID) SCHEME

In [18], [19], the symmetric property of the PSSS is exploited to decouple the detection of the SSID from the IFO recovery task so that they can be detected sequentially. To aim this, the received PSSS is normalized to remove the effect of the channel fading, leading to the channel-compensated objective function as follows [19]

$$\Phi_b(m) = \frac{1}{N_p/2-1} \sum_{k\in\mathcal{D}^+} \tilde{Y}_l(k+m)\tilde{Y}_l(-k+m+1) \tag{11}$$

where $\mathcal{D}^+ = \{k | 2 \le k \le N_p/2\}$ is the set of positive subcarrier indices of differential PSSS and $\tilde{Y}_l(k) = \bar{Y}_l(k)/|\bar{Y}_l(k)|$. If $m = \epsilon$, the function $\Phi_b(m)$ tends to approach one. Since $\Phi_b(m)$ is independent of ZC index u_i, the SSID-independent IFO estimation is performed as

$$\hat{\epsilon} = \underset{|m|\le M}{\arg\min} \, |\Phi_b(m) - 1| \, . \tag{12}$$

Since $\Phi_b(m)$ is independent of ZC index u_i, the SSID is sequentially detected with a reduced search space of size 2

$$\hat{n} = \underset{n\in\{0,1\}}{\arg\max} \ \Re\{\Phi_c(n)\} \tag{13}$$

where

$$\Phi_c(n) = \sum_{k\in\mathcal{D}^+} \{\tilde{Y}_l(k+\hat{\epsilon}) + \tilde{Y}_l^*(-k+\hat{\epsilon}+1)\}D_n^*(k). \tag{14}$$

The disadvantage of the SISID method is that the effect of STO is doubled compared to (9).

IV. PROPOSED IFO AND SSID DETECTION SCHEME

This section presents a robust and computationally efficient joint detection scheme using inherent property of the synchronization signal in the LTE-D2D system. The differential correlation is used to remove the effect of channel fading and then differential PSSS subcarriers are grouped to form the basis for low-complexity detection. As a performance indicator of the proposed joint detector, the probability of detection failure is theoretically derived.

A. ALGORITHM DESCRIPTION

We present possible simplifications to reduce the implementation complexity by partitioning the set $\mathcal{D}^+$ having $N_p/2-1$ differential PSSS subcarriers into N_s subsets. Thus, each PSSS subcarrier belongs to a subset with an acceptable phase difference. With this strategy in mind, the g-th subset can be constructed to meet the following condition

$$\mathcal{D}_g = \left\{ k \left| \, |\arg\{D_n(k_g)D_n^*(k)\}| \le \theta + \frac{p\pi}{2} \right. \right\}, \quad p = 0, 1, 2, 3 \tag{15}$$

where $\arg\{\cdot\}$ is the phase of its argument, k_g denotes the representative subcarrier in subset g, and θ is an angle threshold that controls the similarity between differential PSSS subcarriers in each subset. Since $D_0(k) = D_1^*(k)$, one can readily expect that two PSSS signals $D_0(k)$ and $D_1(k)$ have the same subset configuration. The purpose of subset partitioning is to ensure that the phase difference between the representative PSSS subcarrier and remaining subcarriers in subset is in the range $[-\theta, \theta]$ after being rotated by $p\pi/2$.

The PSSS subset partitioning is iteratively repeated until $N_p/2-1$ differential PSSS subcarriers are assigned to one of the subsets. The complete procedure is as follows:

Step 1): Initialize an index of PSSS subset by $g = 1$ and $\bar{\mathcal{D}} \leftarrow \mathcal{D}^+$.

Step 2): Determine the first subcarrier index in the g-th PSSS subset $k_g = \min\{\bar{\mathcal{D}}\}$, where $\min\{\bar{\mathcal{D}}\}$ returns the minimum value of set $\bar{\mathcal{D}}$.

Step 3): Construct the g-th PSSS subset $\mathcal{D}_g$ that satisfies the condition (15).

Step 4): Set $\bar{\mathcal{D}} = \bar{\mathcal{D}} \setminus \mathcal{D}_g$.

Step 5): If $\bar{\mathcal{D}} = \varnothing$ then $N_s = g$ and stop, otherwise $g = g+1$ and go to step 2.

Based on the subset partitioning described above, the in-phase rotated objective function is computed as

$$\Phi_d(m, n) = \sum_{g=1}^{N_s} D_n^*(k_g) \sum_{k\in\mathcal{D}_g} W_n(k)\hat{Y}_l(k+m) \tag{16}$$

where $\hat{Y}_l(k+m) = \bar{Y}_l(k+m) + \bar{Y}_l^*(-k+m+1)$, $W_n(k) \in \{\pm 1, \pm j\}$ is the conversion indicator that makes the phase difference between the representative PSSS subcarrier $D_n(k_g)$ and $D_n(k)$ in $k \in \mathcal{D}_g$ to be within $[-\theta, \theta]$. Note that $W_n(k)$ is beneficial in terms of implementation because it is performed without multiplication. The number of differential PSSS subcarriers in subset g is denoted by N_g and thus $\sum_{g=1}^{N_s} N_g = N_p/2 - 1$.

When $m = \epsilon$ and $n = i$, substituting (7) into (16) yields

$$\Phi_d(m,n) = \sum_{g=1}^{N_s} \sum_{k\in\mathcal{D}_g} \mathcal{H}_n(k) D_n^*(k) + \sum_{g=1}^{N_s} \sum_{k\in\mathcal{D}_g} W_n(k)\mathcal{H}_n(k)\xi_n^*(k) + \sum_{g=1}^{N_s} \sum_{k\in\mathcal{D}_g} \hat{Z}_l(k) \tag{17}$$

where $\xi_n(k) = D_n(k_g) - W_n(k)D_n(k)$ is the difference between the first PSSS subcarrier and other in-phase rotated PSSS subcarriers in subset g, $\hat{Z}_l(k) = W_n(k)\{\bar{Z}_l(k) + \bar{Z}_l^*(-k+1)\}D_n^*(k_g)$, and

$$\begin{aligned}\mathcal{H}_n(k+m-\epsilon) = {} & |H_l(k+m-\epsilon)|^2 D_n(k+m-\epsilon)e^{j\tau\rho} \\ & + |H_l(-k+1+m-\epsilon)|^2 \\ & \times D_n^*(-k+1+m-\epsilon)e^{-j\tau\rho}.\end{aligned} \tag{18}$$

As can be seen from (17), the objective function is affected by the STO-induced phase rotation and the difference between PSSS subcarriers in subset even as the signal-to-noise ratio (SNR) goes to infinity. Assuming that $D_n(k)$'s are statistically independent for different n's and k's, the central limit theorem ensures that the probability density function of the second term on the right hand side of (17) follows a zero-mean Gaussian distribution. Thus, using $D_n(k) = D_n^*(-k+1)$, it follows that

$$\begin{aligned}\mathbb{E}\{\Phi_d(m,n)\} = \sum_{g=1}^{N_s} \sum_{k\in\mathcal{D}_g} \{ & |H_l(k)|^2 e^{j\tau\rho} \\ & \times |H_l(-k+1)|^2 e^{-j\tau\rho}\} E_P^2\end{aligned} \tag{19}$$

where $\mathbb{E}\{\cdot\}$ denotes the expectation and $E_P = |P_i(k)|^2$. If $m \neq \epsilon$, $\Phi_d(m,n)$ takes expression

$$\begin{aligned}\Phi_d(m,n) = {} & \sum_{g=1}^{N_s} \sum_{k\in\mathcal{D}_g} \mathcal{H}_i(k+m-\epsilon) D_n^*(k) \\ & + \sum_{g=1}^{N_s} \sum_{k\in\mathcal{D}_g} W_n(k)\mathcal{H}_i(k+m-\epsilon)\xi_n^*(k) \\ & + \sum_{g=1}^{N_s} \sum_{k\in\mathcal{D}_g} \hat{Z}_l(k), \quad i = 0, 1.\end{aligned} \tag{20}$$

which can be similarly assumed to be zero-mean Gaussian random variable. Consequently, the maximization of $\Phi_d(m,n)$ with respect to (m,n) will give the SSID and IFO as follows

$$(\hat{\epsilon}, \hat{n}) = \underset{|m|\leq M, n\in\{0,1\}}{\arg\max} \ \Re\{\Phi_d(m,n)\}. \tag{21}$$

B. PROBABILITY OF DETECTION FAILURE

Upon successful completion of joint detection of the SSID and IFO, the UE can proceed the SSSS detection. Thus, the overall probability of detection failure $P_f = \text{Prob}\{\hat{\epsilon} \neq \epsilon, \hat{n} \neq i\}$ is considered as a performance measure. In this section, we compute the overall probability of detection failure of the proposed joint estimator when $\tau = 0$ and AWGN channel is considered. Under the hypothesis that $m = \epsilon$ and $n = i$, the distribution of $\Re\{\Phi_d(m,n)\}$ is Gaussian with mean $\mu = (N_p - 2)E_P^2$ and variance

$$\sigma_1^2 = 2E_P^4 \sum_{g=1}^{N_s} \sum_{k\in\mathcal{D}_g} |\xi_n(k)|^2 + (N_p - 2)E_P^2\sigma_Z^2(E_P + \sigma_Z^2/2). \tag{22}$$

When $m \neq \epsilon$, a random variable $\Re\{\Phi_d(m,n)\}$ has a zero-mean Gaussian distribution with variance given by

$$\begin{aligned}\sigma_0^2 = {} & (N_p - 2)E_P^4/2 + E_P^4 \sum_{g=1}^{N_s} \sum_{k\in\mathcal{D}_g} |\xi_n(k)|^2 \\ & + (N_p - 2)E_P^2\sigma_Z^2(E_P + \sigma_Z^2/2).\end{aligned} \tag{23}$$

For equally likely IFOs, letting $z = \Re\{\Phi_d(m,n)\}$, the overall probability of correct detection $\text{Prob}\{\hat{\epsilon} = \epsilon, \hat{n} = i\}$ can be expressed as

$$P_d = \int_{-\infty}^{\infty} \frac{1}{\sqrt{2\pi}} e^{-\frac{z^2}{2}} \left[1 - Q\left(\frac{\sigma_1}{\sigma_0}z + \frac{\mu}{\sigma_0}\right)\right]^{4M+1} dz \tag{24}$$

where $Q(\cdot)$ denotes the Q-function,

$$\frac{\sigma_1^2}{\sigma_0^2} = \frac{1/\gamma + 1/2\gamma^2 + 2P_e/(N_p-2)}{1/2 + 1/\gamma + 1/2\gamma^2 + P_e/(N_p-2)} \tag{25}$$

and

$$\frac{\mu^2}{\sigma_0^2} = \frac{N_p - 2}{1/2 + 1/\gamma + 1/2\gamma^2 + P_e/(N_p-2)} \tag{26}$$

with

$$P_e = \sum_{g=1}^{N_s} \sum_{k\in\mathcal{D}_g} |\xi_n(k)|^2 \tag{27}$$

and $\gamma = E_P/\sigma_Z^2$ being the SNR. For derivation of the closed form, it is convenient to use a tight upper bound of $Q(\cdot)$ expressed as [23]

$$Q\left(\frac{\sigma_1}{\sigma_0}z + \frac{\mu}{\sigma_0}\right) \leq \frac{1}{12} e^{-\frac{1}{2}\left(\frac{\sigma_1}{\sigma_0}z + \frac{\mu}{\sigma_0}\right)^2} + \frac{1}{4} e^{-\frac{2}{3}\left(\frac{\sigma_1}{\sigma_0}z + \frac{\mu}{\sigma_0}\right)^2}. \tag{28}$$

The overall probability of detection failure is given by $P_f = 1 - P_d$. Using multinomial theorem, the upper bound of P_f is obtained as

$$P_f \le 1 - \sum_{v_1+v_2+v_3=4M+1} \left(-\frac{1}{12}\right)^{v_1} \left(-\frac{1}{4}\right)^{v_2} \binom{4M+1}{v_1, v_2, v_3} \cdot \underbrace{\frac{1}{\sqrt{2\pi}} \int_{-\infty}^{\infty} e^{-\frac{z^2}{2}} e^{-\left(\frac{\sigma_1}{\sigma_0} z + \frac{\mu}{\sigma_0}\right)^2 \left(\frac{v_1}{2} + \frac{2v_2}{3}\right)} dz}_{P(v_1, v_2)} \quad (29)$$

where $0 \le v_i \le 4M+1$ $(i = 1, 2, 3)$ and multinomial coefficient is given by

$$\binom{4M+1}{v_1, v_2, v_3} = \frac{(4M+1)!}{v_1! v_2! v_3!}. \quad (30)$$

From [24], $P(v_1, v_2)$ is expressed in a closed form

$$P(v_1, v_2) = \left(1 + \frac{v_1\sigma_1^2}{\sigma_0^2} + \frac{4v_2\sigma_1^2}{3\sigma_0^2}\right)^{-1/2} \cdot e^{-\frac{\mu^2}{2\sigma_1^2}\left\{1 - \left(1 + \frac{v_1\sigma_1^2}{\sigma_0^2} + \frac{4v_2\sigma_1^2}{3\sigma_0^2}\right)^{-1}\right\}}. \quad (31)$$

Plugging (31) into (29) produces

$$P_f \le 1 - \sum_{v_1+v_2+v_3=4M+1} \left(-\frac{1}{12}\right)^{v_1} \left(-\frac{1}{4}\right)^{v_2} \binom{4M+1}{v_1, v_2, v_3} \cdot \left(1 + \frac{v_1\sigma_1^2}{\sigma_0^2} + \frac{4v_2\sigma_1^2}{3\sigma_0^2}\right)^{-1/2} e^{-\frac{\mu^2}{2\sigma_1^2}\left\{1 - \left(1 + \frac{v_1\sigma_1^2}{\sigma_0^2} + \frac{4v_2\sigma_1^2}{3\sigma_0^2}\right)^{-1}\right\}}. \quad (32)$$

It is worthwhile mentioning that the performance when $P_e = 0$ in (24)-(26) coincides with that of the JISID scheme.

C. COMPUTATIONAL COMPLEXITY

The complexity of the detection schemes is evaluated with respect to the number of real floating point operations (flops) considering joint detection scenarios. We assume that one complex multiplication and one complex addition are equal to six and two real flops, respectively [25]. Furthermore, it is assumed that one absolute operation corresponds to three real flops and the quantities $D_n(k)$'s have been pre-calculated. To compute the shifted differential correlations $\bar{Y}_l(k+m)$'s and $\bar{Y}_l(-k+m+1)$'s, it requires $N_p + 2M - 1$ complex multiplications for hypotheses $|m| \le M$. For fair comparison, we count only the number of flops used to get $\Re\{\Phi_a(m,n)\}$ and $\Re\{\Phi_c(n)\}$, respectively. In (9), $4N_p - 9$ real flops are required to calculate $\Re\{\Phi_a(m,n)\}$. Therefore, the total number of real flops required to compute (10) is $12M + 6N_p - 6 + (4M+2)(4N_p - 9)$. Since the absolute operation demands both real and imaginary parts of $\Phi_b(m)$, $8N_p - 13$ real flops are needed to compute $|\Phi_b(m) - 1|$. Thus, (12) requires $12M + 6N_p - 6 + (2M+1)(8N_p - 13)$ real flops. Additionally, $6N_p - 14$ real flops are required for $\Re\{\Phi_c(n)\}$. In the case of the proposed scheme, (16) requires $N_p + 2N_s - 3$ real flops for each m. Considering $4M+2$ hypotheses, the number of total real flops is $12M + 6N_p - 6 + (4M+2)(N_p + 2N_s - 3)$.

TABLE 1. Subset configuration when $\theta = \pi/18$.

g	$\mathcal{D}_g$					
1	2	5	19	22	25	
2	3	6	20	23	26	
3	4	7	21	24	27	
4	8	11	14	17	28	31
5	9	12	15	18	29	
6	10	13	16	30		

TABLE 2. Subset configuration when $\theta = \pi/9$.

g	$\mathcal{D}_g$									
1	2	5	8	11	16	19	22	25	28	31
2	3	6	9	12	14	17	20	23	26	29
3	4	7	10	13	15	18	21	24	27	30

V. SIMULATION RESULTS

The performance of the proposed detection method is evaluated in the LTE network that consists of 15kHz subcarrier spacing and 5MHz bandwidth. The carrier center frequency is 2GHz, the sampling time instant is $T_s = 1/7.68\ \mu s$, the FFT size is $N = 512$, and the GI length is $N_g = 128$. For data transmission, QPSK modulation is used. We adopt two 3D channel models such as indoor hotspot (InH) and urban micro cell (UMi), which are characterized by a maximum excess delay of $0.225\mu s$ and $0.73\mu s$, respectively [26]. Considering the low mobility and the stability of oscillators for D2D applications [3], the IFO is uniformly distributed over $[-2, 2]$, which corresponds to $M = 2$, and the STO is randomly generated from $[0, \tau]$ in samples, where τ is a maximum STO.

To fully implement (16), we have to know the subset configuration characterized by $\mathcal{D}_g$, which is determined depending on angle threshold θ. Since the two differential PSSSs have the relation $D_0(k) = D_1^*(k)$, it can be readily shown that the subset configuration for both u_0 and u_1 is identical for a given θ. By search of all possible combinations considering the number of differential PSSS subcarrieres, it is obtained that $N_s = 10$ for $\theta = \pi/36$, $N_s = 6$ for $\theta = \pi/18$, $N_s = 3$ for $\theta = \pi/9$, and $N_s = 1$ for $\theta = \pi$. In the following, we use three representative subsets: (S1) $\theta = \pi/18$, (S2) $\theta = \pi/9$, and (S3) $\theta = \pi$. Tables 1 and 2 show the subset configuration when $\theta = \pi/18$ and $\theta = \pi/9$, respectively.

First, we perform the simulation to prove the exactness of the numerical analysis. For this purpose, we consider the situation where the STO is perfectly compensated, i.e. $\tau = 0$. Fig. 1 presents the overall probability of detection failure incurred in jointly estimating the SSID and IFO in the AWGN channel. The performance of the conventional schemes is compared with that of the proposed algorithm parameterized by θ. From Fig. 1, we observe that theoretical analysis (symbols) obtained using the upper bound in (32) exactly matches simulated results (lines) irrelevant to subset configuration where there is no STO. As expected, the approximation (28) provides a very tight bound, which becomes more accurate as the SNR grows.

Fig. 2 depicts the overall probability of detection failure of the proposed and conventional estimators when $\tau = 20$,

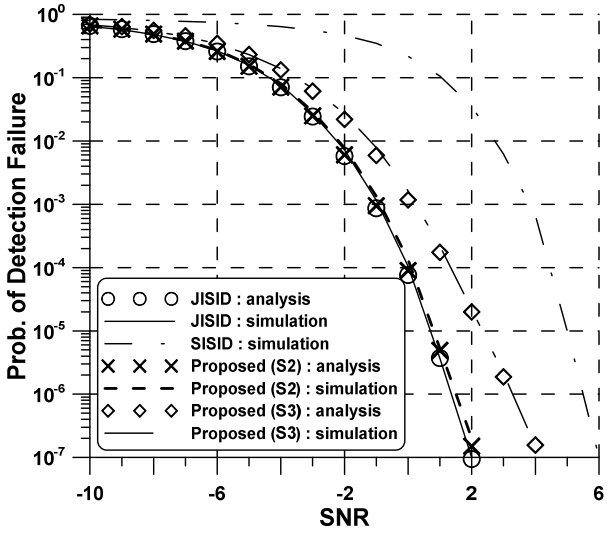

FIGURE 1. Performance of the proposed and conventional detection schemes versus SNR in the AWGN channel when $\tau = 0$.

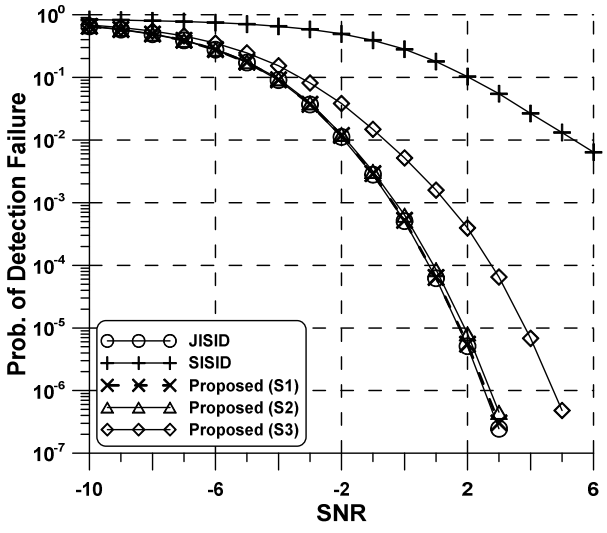

FIGURE 2. Performance of the proposed and conventional detection schemes versus SNR in the AWGN channel when $\tau = 20$.

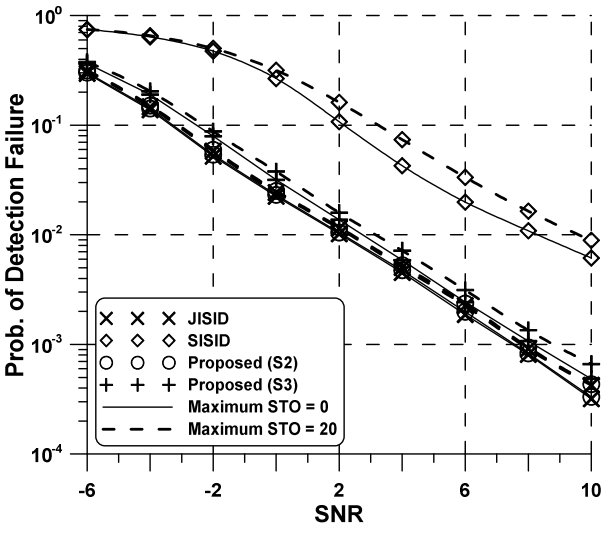

FIGURE 3. Performance of the proposed and conventional detection schemes versus SNR in the InH channel.

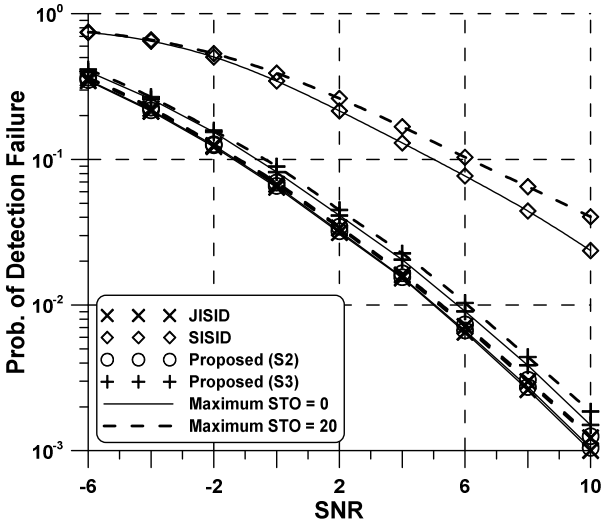

FIGURE 4. Performance of the proposed and conventional detection schemes versus SNR in the UMi channel.

under the same simulation scenarios to Fig. 1. Immediately, one can see that the trend of the curves is similar to that in Fig. 1. More importantly, it can be seen that the accuracy of the JISID scheme and the proposed scheme with subsets 1 and 2 is almost the same in the presence of STO. As the design parameter θ becomes larger, it is expected that the proposed scheme slightly increases the required SNR. However, a maximum SNR loss of the proposed method over the JISID scheme is less than 2dB since the use of subset 3 in the proposed scheme is the worst case scenario where only one representative PSSS subcarrier is present.

Figs. 3 and 4 depict the overall probability of detection failure of the joint detectors in the InH and UMi channels, respectively. It is obvious that the probability of the detection methods is heavily influenced by the amount of frequency selectivity in the presence of STO. This phenomenon becomes more pronounced when the SISID method is used. This is because that the impact of STO is double in the process of computing $\Phi_b(m)$, compared to the JISID scheme and the proposed scheme. It can be seen that the loss of the proposed scheme using the subset 2 with respect to the JISID scheme is negligible at all considered SNR values, whereas 62.6% and 67.1% complexity saving can be achieved against the JISID and SISID schemes, respectively. In the frequency selective fading channel, the performance difference between the JISID scheme and the proposed scheme using the subset 3 is less than 1dB.

VI. CONCLUSION

To achieve a reliable synchronization in LTE-D2D networks, it is important to perform joint detection of SSID and IFO with reduced complexity and high accuracy. To address this problem, an efficient SSID and IFO estimation scheme was

proposed in the LTE assisted D2D communication network. The differential correlation was used for the purpose of joint detection and differential PSSS subcarriers were grouped to form the basis for reduced-complexity estimation. The grouping of the PSSS subcarriers has been found to play an important role on reducing the number of multiplications. Performance analysis was carried out to show how design parameters affect the detection probability and to make a trade-off between the performance and complexity. Simulation results confirmed that the proposed detection scheme achieves robust detection performance with significantly reduced computational load, compared to the conventional detection methods, making it suitable for the LTE-D2D devices.

REFERENCES

[1] *LTE; Evolved Universal Terrestrial Radio Access (E-ULTRA) Physical Channels and Modulation*, document 3GPP TS 36.211 version 13.1.0 Release 13, 2016.

[2] R. I. Ansari, C. Chrysostomou, S. A. Hassan, M. Guizani, S. Mumtaz, J. Rodriguez, and J. J. P. C. Rodrigues, "5G D2D networks: Techniques, challenges, and future prospects," *IEEE Syst. J.*, vol. 12, no. 4, pp. 3970–3984, Dec. 2018.

[3] C. Sexton, Q. Bodinier, A. Farhang, N. Marchetti, F. Bader, and L. A. DaSilva, "Enabling asynchronous machine-type D2D communication using multiple waveforms in 5G," *IEEE Internet Things J.*, vol. 5, no. 2, pp. 1307–1322, Apr. 2018.

[4] Y. Hassan, F. Hussain, S. Hossen, S. Choudhury, and M. M. Alam, "Interference minimization in D2D communication underlaying cellular networks," *IEEE Access*, vol. 5, pp. 22471–22484, Oct. 2017.

[5] G. G. Girmay, Q.-V. Pham, and W.-J. Hwang, "Joint channel and power allocation for device-to-device communication on licensed and unlicensed band," *IEEE Access*, vol. 7, pp. 22196–22205, Feb. 2019.

[6] O. Bello and S. Zeadally, "Intelligent device-to-device communication in the Internet of Things," *IEEE Syst. J.*, vol. 10, no. 3, pp. 1172–1182, Sep. 2016.

[7] A. Ali and W. Hamouda, "On the cell search and initial synchronization for NB-IoT LTE systems," *IEEE Commun. Lett.*, vol. 21, no. 8, pp. 1843–1846, Aug. 2017.

[8] F. Berggren and B. M. Popović, "Primary synchronization signal for D2D communications in LTE-advanced," *IEEE Commun. Lett.*, vol. 19, no. 7, pp. 1241–1244, Jul. 2015.

[9] A. Golnari, M. Shabany, A. Nezamalhosseini, and G. Gulak, "Design and implementation of time and frequency synchronization in LTE," *IEEE Trans. Very Large Scale Integr. (VLSI) Syst.*, vol. 23, no. 12, pp. 2970–2982, Dec. 2015.

[10] N. M. Balasubramanya, L. Lampe, G. Vos, and S. Bennett, "On timing reacquisition and enhanced primary synchronization signal (ePSS) design for energy efficient 3GPP LTE MTC," *IEEE Trans. Mobile Comput.*, vol. 16, no. 8, pp. 2292–2305, Aug. 2017.

[11] N. M. Balasubramanya, L. Lampe, G. Vos, and S. Bennett, "Low SNR uplink CFO estimation for energy efficient IoT using LTE," *IEEE Access*, vol. 4, pp. 3936–3950, Jul. 2016.

[12] M. R. Sriharsha, S. Dama, and K. Kuchi, "A complete cell search and synchronization in LTE," *EURASIP J. Wireless Commun. Netw.*, vol. 2017, p. 101, Dec. 2017.

[13] M. H. Nassralla, M. M. Mansour, and L. M. A. Jalloul, "A low-complexity detection algorithm for the primary synchronization signal in LTE," *IEEE Trans. Veh. Technol.*, vol. 65, no. 10, pp. 8751–8757, Oct. 2016.

[14] Z. Zhang, J. Liu, and K. Long, "Low-complexity cell search with fast PSS identification in LTE," *IEEE Trans. Veh. Technol.*, vol. 61, no. 4, pp. 1719–1729, May 2012.

[15] J.-C. Lin, Y.-T. Sun, and H. V. Poor, "Initial synchronization exploiting inherent diversity for the LTE sector search process," *IEEE Trans. Wireless Commun.*, vol. 15, no. 2, pp. 1114–1128, Feb. 2016.

[16] S.-L. Su, Y.-C. Lin, and Y.-J. Fan, "Joint sector identity and integer part of carrier frequency offset detection by phase-difference in long term evolution cell search process," *IET Commun.*, vol. 7, no. 10, pp. 950–959, Jul. 2013.

[17] M. Morelli and M. Moretti, "A robust maximum likelihood scheme for PSS detection and integer frequency offset recovery in LTE systems," *IEEE Trans. Wireless Commun.*, vol. 15, no. 2, pp. 1353–1363, Feb. 2016.

[18] W.-J. Shin, H. Yang, S. Lee, and Y.-H. You, "Complexity effective integer frequency offset and sector cell detection scheme for LTE downlink system," *Wireless Pers. Commun.*, vol. 75, no. 4, pp. 2371–2381, Apr. 2014.

[19] C.-Y. Chu, I.-W. Lai, Y.-Y. Lan, and T.-D. Chiueh, "Efficient sequential integer CFO and sector identity detection for LTE cell search," *IEEE Commun. Lett.*, vol. 3, no. 4, pp. 389–392, Aug. 2014.

[20] F. J. López-Martínez, E. Martos-Naya, and J. T. Entrambasaguas, "Low complexity cell search scheme for LTE and LTE-advanced mobile technologies," *Comput. Elect. Eng.*, vol. 38, no. 6, pp. 1502–1512, 2012.

[21] J. Myung, J. Kang, Y. Baek, and B. Koo, "Efficient S-SCH detection algorithm for LTE downlink channel," *IEEE Trans. Veh. Technol.*, vol. 63, no. 6, pp. 2969–2973, Jul. 2014.

[22] M. Morelli and M. Moretti, "A maximum likelihood approach for SSS detection in LTE systems," *IEEE Trans. Wireless Commun.*, vol. 16, no. 4, pp. 2423–2433, Apr. 2017.

[23] M. Chiani, D. Dardari, and M. K. Simon, "New exponential bounds and approximations for the computation of error probability in fading channels," *IEEE Trans. Wireless Commun.*, vol. 2, no. 4, pp. 840–845, Jul. 2003.

[24] I. S. Gradshteyn and I. M. Ryzhik, *Table of Integrals, Series, and Products*, 8th ed. New York, NY, USA: Academic, 2014.

[25] G. H. Golub and C. F. Van Loan, *Matrix Computations*. Baltimore, MD, USA: Johns Hopkins Univ. Press, 1996.

[26] *Guidelines for Evaluation of Radio Interface Technologies for IMT-Advanced*, document ITU-R M.2135-1, 2009.

YONG-AN JUNG received the B.S., M.S., and Ph.D. degrees from the Department of Computer Engineering, Sejong University, Seoul, South Korea, in 2011, 2013, and 2019, respectively.

He is currently a Postdoctoral Researcher with Sejong University. His research interests include the areas of wireless/wired communications systems design, spread spectrum transceivers, and system architecture, especially for realizing advanced orthogonal frequency-division multiplexing (OFDM) communications systems.

JONG-HONG PARK received the B.S. and Ph.D. degrees in electrical and electronic engineering from Yonsei University, Seoul, South Korea, in 2010 and 2016, respectively.

Since 2017, he has been a Senior Researcher with the Autonomous IoT Research Center, Korea Electronics Technology Institute, South Korea. His research interests include the areas of wireless communication technologies and the Internet of Things (IoT) platform design for multiple UAV operation systems.

YOUNG-HWAN YOU received the B.S., M.S., and Ph.D. degrees in electronic engineering from Yonsei University, Seoul, South Korea, in 1993, 1995, and 1999, respectively.

From 1999 to 2002, he was a Senior Researcher with Wireless PAN Technology Project Office, Korea Electronics Technology Institute, South Korea. Since 2002, he has been a Professor with the Department of Computer Engineering, Sejong University, Seoul. His research interests include the field of wireless communications and signal processing with particular focus on wireless communications systems design, spread spectrum transceivers, and system architecture for realizing advanced digital communications systems, especially for wireless orthogonal frequency-division multiplexing (OFDM).